



1 **Uncertainty analysis of a European high-resolution emission**
2 **inventory of CO₂ and CO to support inverse modelling and**
3 **network design**

4 Ingrid Super¹, Stijn N.C. Dellaert¹, Antoon J.H. Visschedijk¹, Hugo A.C. Denier van der Gon¹

5 ¹Department of Climate, Air and Sustainability, TNO, P.O. Box 80015, 3508 TA Utrecht, Netherlands

6 *Correspondence to:* Ingrid Super (ingrid.super@tno.nl)



7 **Abstract.** Quantification of greenhouse gas emissions is receiving a lot of attention, because of its relevance for
8 climate mitigation. Quantification is often done with an inverse modelling framework, combining atmospheric
9 transport models, prior gridded emission inventories and a network of atmospheric observations to optimize the
10 emission inventories. An important aspect of such method is a correct quantification of the uncertainties in all
11 aspects of the modelling framework. The uncertainties in gridded emission inventories are, however, not
12 systematically analysed. In this work, a statistically coherent method is used to quantify the uncertainties in a
13 high-resolution gridded emission inventory of CO₂ and CO for Europe. We perform a range of Monte Carlo
14 simulations to determine the effect of uncertainties in different inventory components, including the spatial and
15 temporal distribution, on the uncertainty in total emissions and the resulting atmospheric mixing ratios. We find
16 that the uncertainty in the total emissions for the selected domain are 1 % for CO₂ and 6 % for CO. Introducing
17 spatial disaggregation causes a significant increase in the uncertainty of up to 40 % for CO₂ and 70 % for CO for
18 specific grid cells. Using gridded uncertainties specific regions can be defined that have the largest uncertainty in
19 emissions and are thus an interesting target for inverse modelers. However, the largest sectors are usually the best-
20 constrained ones (low relative uncertainty), so the absolute uncertainty is the best indicator for this. With this
21 knowledge areas can be identified that are most sensitive to the largest emission uncertainties, which supports
22 network design.



23 **1 Introduction**

24 Carbon dioxide (CO₂) is the most important greenhouse gas and is emitted in large quantities from human
25 activities, especially from the burning of fossil fuels (Berner, 2003). A reliable inventory of fossil fuel CO₂
26 (FFCO₂) emissions is important to increase our understanding of the carbon cycle and how the global climate will
27 develop in the future. The impact of CO₂ emissions is visible on a global scale and international efforts are required
28 to mitigate climate change, but cities are the largest contributors to FFCO₂ emissions (about 70% (IEA, 2008)).
29 Therefore, emissions should be studied at different spatial and temporal scales to get a full understanding of their
30 variability and mitigation potential.

31 One way of describing emissions is an emission inventory, which is a structured set of emission data,
32 distinguishing different pollutants and source categories. Often, emission inventories are based on reported
33 country-level emission data (for example from the National Inventory Reports (NIR's)), which are spatially and
34 temporally disaggregated (scaled-down) to a certain level using proxies (e.g. the TNO inventories (Denier van der
35 Gon et al., 2017; Kuenen et al., 2014)). Other emission inventories are based on local energy consumption data
36 and reported emissions aggregated to the required spatial scale (scaled-up) (e.g. Hestia (Gurney et al., 2011, 2019))
37 or rely on (global) statistical data and a consistent set of (non-country specific) emission factors representing
38 different technology levels (e.g. EDGAR (<http://edgar.jrc.ec.europa.eu>)). Most inventories, including the one used
39 in this study, rely on a combination of methods, using large-scale data supplemented with local data. Gridded
40 emission inventories are essential as input for atmospheric transport models to facilitate comparison with
41 observations of CO₂ concentrations, as well as in inverse modelling as a prior estimate of the emission locations
42 and magnitude.

43 During the compilation of an emission inventory uncertainties are introduced at different levels (e.g. magnitude,
44 timing or locations) and increasingly more attention is given to this topic. Parties to the United Nations Framework
45 Convention on Climate Change (UNFCCC) report their annual emissions (disaggregated over source sectors and
46 fuel types) in a NIR (UNFCCC, 2019), which includes an assessment of the uncertainties in the underlying data
47 and an analysis of the uncertainties in the total emissions following IPCC (Intergovernmental Panel on Climate
48 Change) guidelines. The simplest uncertainty analysis is based on simple equations for combining uncertainties
49 from different sources (Tier 1 approach). A more advanced approach is a Monte Carlo simulation, which allows
50 for non-normal uncertainty distributions (Tier 2 approach). The Tier 2 approach has been used by several
51 countries, for example Finland (Monni et al., 2004) and Denmark (Fauster et al., 2011).

52 These reports provide a good first step in quantifying emission uncertainties, but the uncertainty introduced by
53 using proxies for spatial and temporal disaggregation are not considered. These are, however, an important source
54 of uncertainty in the gridded emission inventories (Andres et al., 2016). Inverse modelling studies are increasingly
55 focusing on urban areas, the main source areas of FFCO₂ emissions, for which emission inventories with a high
56 spatiotemporal resolution are used to better represent the variability in local emissions affecting local
57 concentration measurements. Understanding the uncertainty at higher resolution than the country-level is thus
58 necessary, which means that the uncertainty caused by spatiotemporal disaggregation becomes important as well.
59 The uncertainties in emission inventories are important to understand for several reasons. First, knowledge of
60 uncertainties helps pinpointing emission sources or areas that require more scrutiny (Monni et al., 2004; Palmer
61 et al., 2018). Second, knowledge of uncertainties in prior emission estimates is an important part of inverse
62 modelling frameworks, which can be used for emission verification and in support of decision-making (Andres et



63 al., 2014). For example, if uncertainties are not properly considered, there is a risk that the uncertainty range does
64 not contain the actual emission value. In contrast, if uncertainties are large the prior gives little information about
65 the actual emissions and more independent observations are needed. Third, emission uncertainties can support
66 atmospheric observation system design, for example for inverse modelling studies. An ensemble of model runs
67 can represent the spread in atmospheric concentration fields due to the uncertainty in emissions. Locations with a
68 large spread in atmospheric concentrations are most sensitive to uncertainties in the emission inventory and are
69 preferential locations for additional atmospheric measurements. To conclude, emission uncertainties are a critical
70 part of emission verification systems and require more attention. To better understand how uncertainties in
71 underlying data affect the overall uncertainty in gridded emissions, a family of ten emission inventories is
72 compiled within the H2020 project CO₂ Human Emissions (CHE). These can be made available upon request.
73 In this paper we illustrate a statistically coherent method to assess the uncertainties in a high-resolution emission
74 inventory, including uncertainties resulting from spatiotemporal disaggregation. For this purpose, we use a Monte
75 Carlo simulation to propagate uncertainties in underlying parameters into the total uncertainty in emissions (like
76 the Tier 2 approach). We illustrate our methodology using a new high-resolution emission inventory for a
77 European zoom region. We illustrate the magnitude of the uncertainties in emissions and how this affects
78 simulated concentrations. The research questions are:

- 79 1) How large are uncertainties in total inventory emissions and how does this differ per sector and country?
- 80 2) How do uncertainties in spatial proxy maps affect local measurements?
- 81 3) How important is the uncertainty in time profiles for the calculation of annual emissions from daytime
82 (12-16h LT) emissions, which result from inverse modelling studies using only daytime observations?
- 83 4) What information can we gain from high-resolution gridded uncertainty maps by comparing different
84 regions?

85 Inverse modelling studies often focus on a single species like CO₂, but co-emitted species are increasingly
86 included to allow source partitioning (Boschetti et al., 2018; Zheng et al., 2019). In this study, we look into CO₂
87 and CO to illustrate our methodology, but the methodology can be applied to other (co-emitted) species.

88 2 Methodology

89 2.1 The high-resolution emission inventory

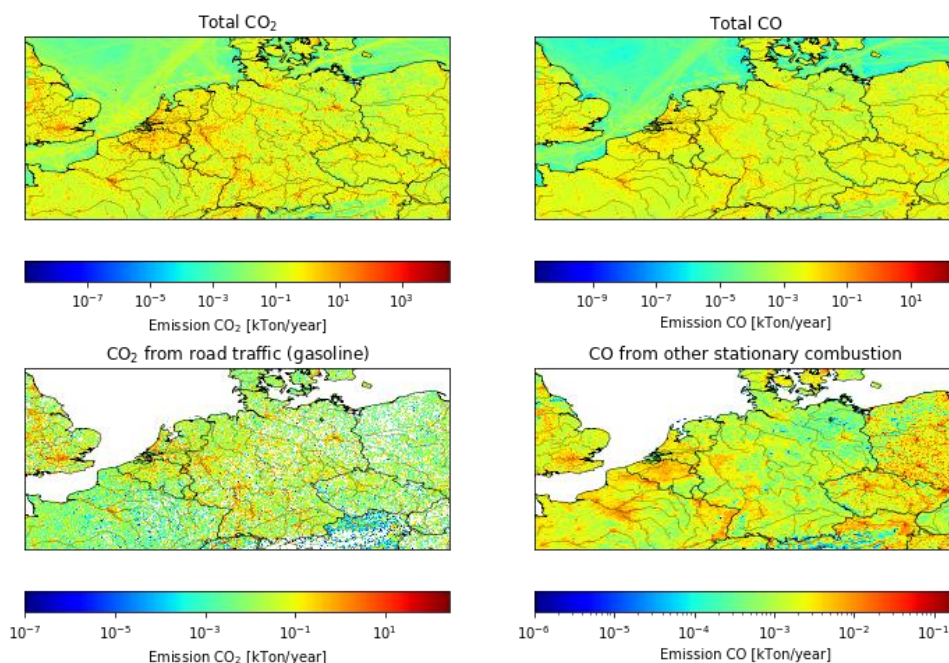
90 **Table 1: Characteristics of the high-resolution emission inventory TNO GHGco v1.0**

Air pollutants	CO _{ff} , CO _{bf} , NO _x
Greenhouse gases	CO ₂ _{ff} , CO ₂ _{bf} , CH ₄
Resolution	1/60° longitude x 1/120° latitude (~ 1x1 km over central Europe)
Period covered	2015 (annual emissions)
Domain	-2° W–19° E, 47° N–56°N
Sector aggregation	GNFR (A to L), with GNFR F (Road Transport) split in F1 to F4 (total 16 sectors)
Countries	Complete: DEU, NLD, BEL, LUX, CZE Partially: GBR, FRA, DNK, AUT, POL, CHE, ITA, SVK and HUN

91
92 The basis of this study is a high-resolution emission inventory for the greenhouse gases CO₂ and CH₄ and the co-
93 emitted tracers CO and NO_x for the year 2015 (TNO GHGco v1.0, see details in Table 1). In this paper we only



94 use CO₂ and CO, which are divided over fossil fuel (ff) and biofuel (bf) emissions (no land use and land use
95 change emissions are included). The emission inventory covers a domain over Europe, including Germany,
96 Netherlands, Belgium, Luxembourg and the Czech Republic, and parts of Great Britain, France, Denmark, Austria
97 and Poland (see also Figure 1).
98 The emission inventory is based on the reported emissions by European countries to the UNFCCC (only
99 greenhouse gases) and to EMEP/CEIP (European Monitoring and Evaluation Programme/Centre on Emission
100 Inventories and Projections, only air pollutants). UNFCCC CO₂ emissions have been aggregated to ~250 different
101 combinations of NFR sectors (Nomenclature For Reporting) and fuel types. EMEP/CEIP CO emissions have been
102 split over the same NFR sector-fuel type combinations by TNO using the GAINS model (Amann et al., 2011)
103 and/or TNO data. In some cases, the data was gap filled, replaced or (dis)aggregated to obtain a consistent dataset.
104 Next, each NFR sector is linked to a high-resolution proxy map (e.g. population density for residential combustion
105 of fossil fuels or AIS data for shipping re-gridded to 1/60° x 1/120°), which is used to spatially disaggregate the
106 reported country-level emissions. Where possible, the exact location and reported emission of large point sources
107 is used (e.g. from the E-PRTR (European Pollutant Release and Transfer Register)). The third step is temporal
108 disaggregation, for which standard time profiles are used (Denier van der Gon et al., 2011). Finally, the gridded
109 emissions are aggregated per GNFR sector (see Table 2) for the emission inventory. The final emission maps of
110 CO₂ and CO are shown in Figure 1, together with two examples of a source sector map. Note that these maps do
111 not clearly show the large point source emissions, while these make up almost 45 % of all CO₂ emissions and 26
112 % of all CO emissions.



113

114 **Figure 1: Total emissions of CO₂ and CO, road traffic (gasoline) emissions of CO₂, and other stationary combustion**
115 **emissions of CO for 2015 in kt yr⁻¹ (defined per grid cell).**



116 2.2 Uncertainties in parameters

117 The emission inventory is used as basis for an uncertainty analysis by assigning an uncertainty to each parameter
118 underlying the UNFCCC-EMEP/CEIP emission inventories and further disaggregation thereof. Although the
119 aggregation to GNFR sectors makes the emission inventory more comprehensible, we use the more detailed
120 underlying data for the uncertainty analysis. The reason is that the uncertainties can vary enormously between
121 sub-sectors and fuel types. Generally, the emission at a certain time and place is determined by four types of
122 parameters: activity data, emission factor, spatial distribution and time profile. The activity data and emission
123 factors are used by countries to calculate their emissions. The spatial proxy maps and time profiles are used for
124 spatiotemporal disaggregation. All uncertainties need to be specified per NFR sector-fuel type combination that
125 is part of the Monte Carlo simulation. In the following sections the steps taken to arrive at a covariance matrix for
126 the Monte Carlo simulation are described. Tables with uncertainty data can be found in the Appendix.

127 **Table 2: Overview of GNFR sectors distinguished in the emission inventory**

GNFR category	GNFR category name
A	A_PublicPower
B	B_Industry
C	C_OtherStationaryComb
D	D_Fugitives
E	E_Solvents
F	F_RoadTransport
G	G_Shipping
H	H_Aviation
I	I_OffRoad
J	J_Waste
K	K_AgriLivestock
L	L_AgriOther
F1	F_RoadTransport_exhaust_gasoline
F2	F_RoadTransport_exhaust_diesel
F3	F_RoadTransport_exhaust_LPG_gas
F4	F_RoadTransport_non-exhaust

128 2.2.1 Parameter selection

129 The first step is to identify which parameters should be included in the Monte Carlo simulation. As mentioned
130 before there are about 250 different combinations of NFR sectors and fuel types and including all of them would
131 be a huge computational challenge. However, a selection of 112 combinations makes up most of the fossil fuel
132 emissions (96 % for CO₂ and 92 % for CO) and therefore a pre-selection was made. This results in a covariance
133 matrix of 224x224 parameters (112 sector-fuel combinations for two species). To further reduce the size of the
134 problem, the emissions are partly aggregated before starting the Monte Carlo for the spatial proxies (mostly fuels
135 are combined per sector, because they have the same spatial distribution). This results in a total of 59 NFR sector-
136 spatial proxy combinations, which are put in a separate covariance matrix. The time profiles are applied to the



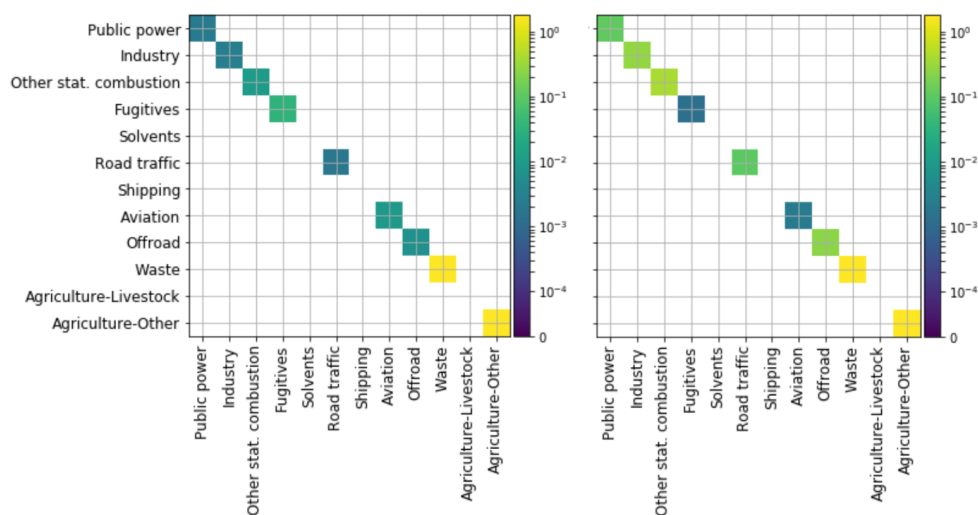
137 aggregated GNFR sectors, which make up the last covariance matrix. Note that the spatial proxies and time
138 profiles are the same for CO₂ and CO, except for the spatially explicit E-PRTR point source data.

139 2.2.2 Uncertainties in reported emissions

140 Country-level emissions are estimated from the multiplication of activity data and emission factors. Activity data
141 consist for the most part of fossil fuel consumption data available from national energy balances. Some fuel
142 consumptions are better known than others and uncertainties vary across sectors. An emission factor is the amount
143 of emission that is produced per unit of activity (e.g. amount of fuel consumed). For CO₂ this depends mainly on
144 the carbon content of the fuel. In contrast, CO emissions are extremely dependent on combustion conditions,
145 certain industrial processes and in-place technologies.

146 The NIR's for greenhouse gases (GHGs) provide a table with uncertainties in activity data and CO₂ emission
147 factors on the level of NFR sector - fuel combinations. The uncertainties reported by each country are averaged
148 to get one uncertainty per NRF sector-fuel combination for the entire domain. Overall, the differences between
149 countries are small. The uncertainties in activity data and CO₂ emission factors are relatively low and normally
150 distributed.

151 The CO emission factors are mostly based on basic uncertainty ranges provided in the EMEP/EEA Guidebook
152 (European Environment Agency, 2016) and supplemented by BAT reference documents from which reported
153 emission factor ranges are taken as uncertainty range (<http://eippcb.jrc.ec.europa.eu/reference/>). The CO emission
154 factor uncertainties are generally expressed by a factor, which means that the highest and lowest limit values are
155 either the specified factor above or below the most common value. Therefore, these uncertainties have a lognormal
156 distribution and are relatively large.



157

158 **Figure 2: Covariance matrices for total emissions of CO₂ (left) and CO (right) per aggregated source sector. A white**
159 **space on the diagonal indicates this sector is not included in the Monte Carlo simulation.**

160 To estimate the overall uncertainty in the emissions per NFR sector-fuel combination, the uncertainties in the
161 activity data and emission factors need to be combined (shown in Figure 2 for the aggregated GNFR sectors).
162 When both uncertainties are of the same order and relatively small, as well as both having a normal distribution,



163 the overall emission uncertainty is calculated with the standard formula for error propagation for non-correlated
164 normally distributed variables (see Sect. 2.4). For most CO emission factors, uncertainties are much higher and
165 have a lognormal distribution instead of normal. In that case the uncertainty of the variable with the highest
166 uncertainty is assumed to be indicative for the overall uncertainty of the emission, which in general means the
167 uncertainty of the CO emission factor determines the overall uncertainty of the CO emission, with the distribution
168 remaining lognormal. The error introduced by fuel type disaggregation for CO is not considered.

169 Finally, for power plants and road traffic we assumed error correlations to exist between different sub-sectors per
170 fuel type, and between different fuel types per sub-sector for other NFR sectors. In some cases, correlations also
171 exist between different NFR sectors belonging to the same GNFR sector. The definition of correlations is
172 important, because they affect the total uncertainties. For example, if emission factors of sub-sectors are
173 correlated, deviations can amplify each other, leading to higher overall uncertainties. In contrast, the division of
174 the well-known total fuel consumption of a sector over its sub-sectors includes an uncertainty which is anti-
175 correlated (i.e. if too much fuel consumption is assigned to one sub-sector, too little is assigned to another). This
176 has little impact on the total emissions, because uncertainties only exist at lower levels.

177 **2.2.3 Uncertainties in spatial proxies**

178 The proxy maps used for spatial disaggregation can introduce a large uncertainty coming from the following
179 sources:

- 180 1) The proxy is not correctly representing real-world locations of what it is supposed to represent, either
181 because there are cells included in which none of the intended activity takes place or cells are missing in
182 which the intended activity does take place (proxy quality).
- 183 2) The proxy is not fully representative for the activity it is assumed to represent, for example if there is a non-
184 linear relationship between the proxy value and the emission (proxy representativeness): a grid cell with
185 twice the population density does not necessarily have double the amount of residential heating emissions,
186 because heating can be more efficient in densely populated areas and/or apartment blocks.
- 187 3) The cell values themselves are uncertain, e.g. the population density or traffic intensity (proxy value).

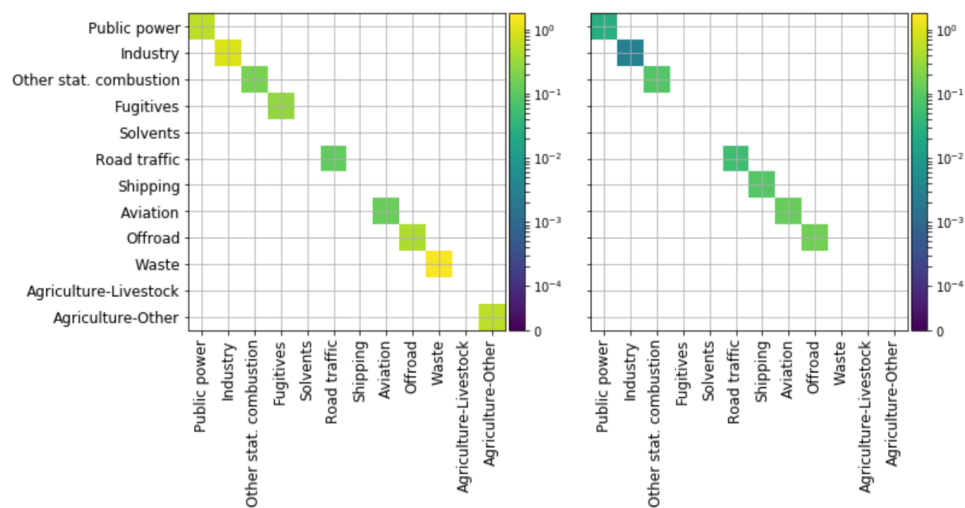
188 We attempt to capture the second and third source of uncertainty in a single numerical indicator representing the
189 uncertainty at cell level (see Figure 3 for the uncertainty per aggregated GNFR sector). The overall uncertainties
190 are based on expert judgement and inevitably include a considerable amount of subjectivity. This type of
191 uncertainty is often large and has a lognormal distribution, except for proxies related to road traffic and some
192 proxies related to commercial/residential emissions sources. We assume no error correlations exist. The first
193 source of uncertainty is also considered in one of the experiments (see Sect. 2.4 for a description of this
194 experiment).

195 **2.2.4 Uncertainties in time profiles**

196 The time profiles currently consist of fixed monthly, daily and hourly fractions that are based on long-term average
197 activity data and/or socio-economic characteristics. These profiles are applied for each year and for the entire
198 domain, considering only time zone differences. In reality, the time profiles can differ between countries, and
199 from year to year. For example, residential emissions are strongly correlated with the outside temperature and



200 therefore show a strong seasonal cycle. However, one winter can be very cold, whereas the next can have above-
 201 average temperatures.



202
 203 **Figure 3: Covariance matrices for spatial proxies (left) and time profiles (right) per aggregated source sector. These**
 204 **are the same for CO₂ and CO. A white space on the diagonal indicates this sector is not included in the Monte Carlo**
 205 **simulation.**

206 To quantify the uncertainty in time profiles, a range of time profiles (for a full year, hourly resolution) was created
 207 for each source sector based on activity data (such as traffic counts). These profiles can be from different years
 208 and countries, so that the full range of possibilities is included. These are compared to the fixed time profiles to
 209 estimate the uncertainties, which are normally distributed (see Figure 3 for the uncertainty per aggregated GNFR
 210 sector). We assume no error correlations exist.

211 **Table 3: Percentage (%) of emissions of CO₂ and CO (fossil + biofuel) that are attributed to large point sources**
 212 **(accounted for in databases) for source sectors public power and industry.**

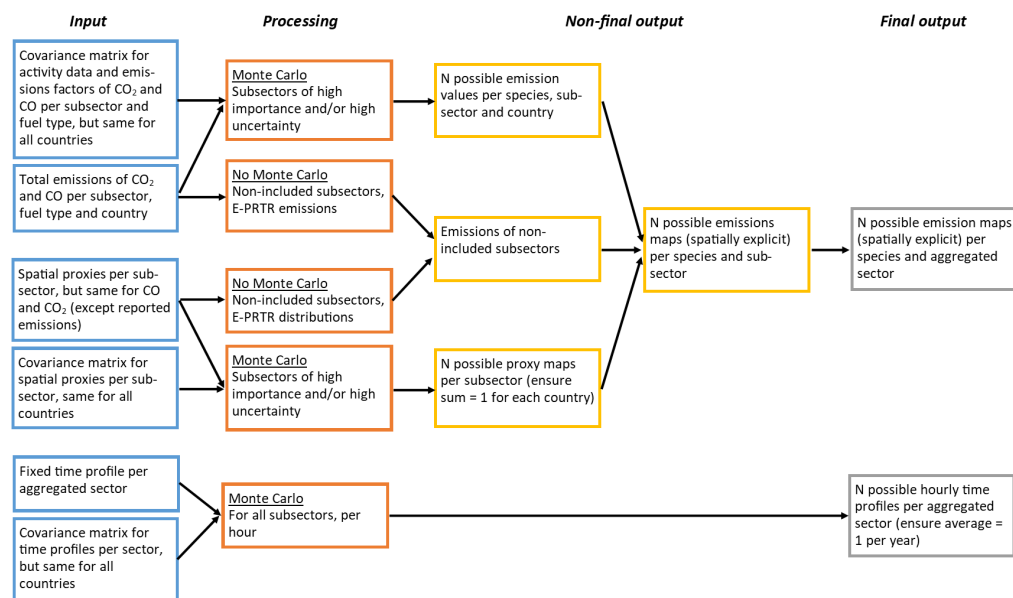
Country	CO ₂		CO	
	Public power	Industry	Public power	Industry
Netherlands	84.3 %	80.4 %	80.7 %	86.0 %
Belgium	65.4 %	77.5 %	99.5 %	93.5 %
Luxembourg	67.1 %	67.2 %	61.8 %	94.2 %
Germany	85.9 %	74.1 %	96.7 %	87.9 %
Czech Republic	89.2 %	90.4 %	79.3 %	94.3 %

213 2.3 The Monte Carlo simulation

214 Within a Monte Carlo simulation we create an ensemble (size N) of emissions, spatial proxies and time profiles
 215 by drawing random samples from the covariance matrices described in Sect. 2.2. This creates a set of possible
 216 solutions in the emission space, reflecting the uncertainties in the underlying parameters. The entire process is
 217 shown in Figure 4. As mentioned before, not all sub-sectors are included in the Monte Carlo simulation and the
 218 non-included emissions are added to each ensemble member at the final stage. Important is to ensure that the time



219 profiles and the spatial proxies do not affect the total emissions, so proxies should sum up to 1 for each country
220 and time profiles should be on average 1 over a full year. Before doing this, negative values are removed.
221 The source sectors that include point source emissions (mainly public power and industry) are treated separately.
222 The large point source emissions and their locations are relatively well-known and available from databases (e.g.
223 from E-PRTR), and therefore not included in the Monte Carlo. The remaining part of the emissions (non-point
224 source or small point sources) from these sectors are distributed using generic proxies (e.g. industrial areas) and
225 are calculated as the difference between the total emissions (activity data x emission factor) and the sum of the
226 point source emissions. If negative emissions result from this subtraction of reported point source emissions, the
227 residual is set to zero. Note that the spatial uncertainty of this residual part is often high. The fraction of the public
228 power and industrial emissions that are attributed to large point sources are shown in Table 3 for several countries.



229

230 **Figure 4: Flow-diagram showing the input, processing and output of the Monte Carlo simulation.**

231 **2.4 Experiments to explore uncertainty propagation**

232 In this paper several experiments are performed to examine the impact of the uncertainties in different parameters
233 on the overall emissions and simulated concentrations:

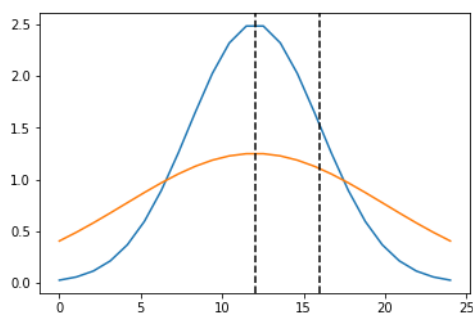
- 234 1) The first experiment uses a MC simulation (N=500) to illustrate the spread in emissions per sector due to
235 uncertainties in emission factors and activity data (no spatial/temporal variability is considered). This
236 experiment is used to show the contribution of specific sectors to the overall uncertainty and to illustrate
237 how uncertainties vary between sectors and countries. For this experiment country totals are used, also for
238 the countries that are partially outside the zoom domain shown in Figure 1. The results are presented in
239 Sect. 3.1.
- 240 2) The second experiment uses a MC simulation (N=500) to illustrate how the uncertainty in spatial proxy
241 maps is translated into uncertainties in simulated concentrations (emissions are taken constant; no temporal
242 variability is included). We use emissions of other stationary combustion (CO₂) and road traffic (CO) to



243 illustrate the importance of having a correct spatial distribution for measurements close to the source area
244 and further away. The results are presented in Sect. 3.2.

245 3) The third experiment compares two spatial proxy maps for distributing ‘residual’ power plant emissions
246 (i.e. those not accounted for in point source databases) to illustrate the potential impact of spreading out
247 small point source emissions when zooming in on small case study areas (emissions are taken constant; no
248 temporal variability is included). The results are presented in Sect. 3.2.

249 4) The fourth experiment uses a MC simulation (N=500) to illustrate the spread in time profiles (emissions are
250 taken constant; no spatial variability is considered). We use this information to determine the error
251 introduced when extrapolating daytime (12–16 h LT) emissions (for example resulting from an inversion)
252 to annual emissions using an incorrect time profile. Figure 5 shows two possible daily cycles, which have
253 46 % (blue) and 25 % (orange) of their emissions between 12 and 16 h LT. Therefore, both time profiles
254 will give a different total daily emission when used to extrapolate the daytime emissions. The results are
255 presented in Sect. 3.3.



256
257 **Figure 5: Schematic overview of two possible time profiles, which represent a different fraction of the total daily**
258 **emissions during the selected period (12–16 h LT, illustrated by the dashed lines).**

259 5) For the final experiment, maps are made of the (absolute and relative) uncertainty in each pixel, including
260 uncertainties in emission factors, activity data and spatial proxies (no temporal variability). For this we used
261 a Tier 1 approach, using the following equations:

$$262 \quad \text{Total relative uncertainty} = \sqrt{\sum \text{standard deviations}^2} / \text{emission sum} \quad (1)$$

263 for the summation of uncorrelation quantities (e.g. sectoral emissions), and:

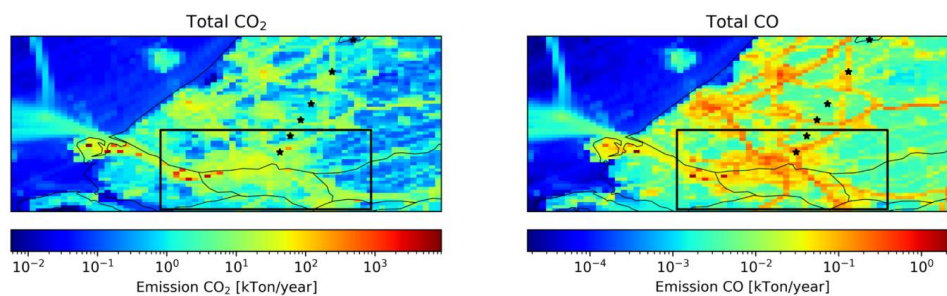
$$264 \quad \text{Total relative uncertainty} = \sqrt{\sum \text{relative uncertainties}^2} \quad (2)$$

265 for the multiplication of random variables, such as used to combine activity data and emission factors. Here,
266 the (total) relative uncertainty is the percentage uncertainty (uncertainty divided by the total) and the
267 standard deviations are expressed in units of the uncertain quantity (percentage uncertainty multiplied with
268 the uncertain quantity). These maps are used to explore spatial patterns in uncertainties and examine what
269 we can learn about different countries or regions. The results are presented in Sect. 3.4.

270 For experiment 2 and 3 a smaller domain is selected to represent a local case study (Figure 6). We used the
271 Rotterdam area, which has been studied in detail before (Super et al., 2017b, 2017a). The domain is about 34x26
272 km and centred over the city, which includes some major industrial activity as well. To translate the emissions
273 into atmospheric concentrations, a simple plume dispersion model is used, the Operational Priority Substances



274 (OPS) model. This model was developed to calculate the transport of pollutants, including chemical
275 transformations (Van Jaarsveld, 2004; Sauter et al., 2016) and was adapted to include CO and CO₂ (Super et al.,
276 2017a). The short-term version of the model calculates hourly concentrations at specific receptor points,
277 considering hourly variations in wind direction and other transport parameters. Although the model is often used
278 for point source emissions, it can also handle surface area sources. This model was chosen because of its very
279 short run time, which makes it suitable for a large ensemble.



280

281 **Figure 6: Emissions of CO₂ and CO for part of the Netherlands, including the sub-domain (black rectangle) over**
282 **Rotterdam. Black stars indicate the receptor locations.**

283 The OPS model is run for each ensemble member for 5 January 2014 from the start of the day until 16 h LT. On
284 this day the wind direction is relatively constant at about 215° and the wind speed is around 6 m s⁻¹. We specify
285 receptor points downwind from the centre of our domain at increasing distance (5, 10, 15, 20, 30 and 40 km). We
286 use the last hour of the simulation for our analyses. We assume emissions from other stationary combustion and
287 road traffic (experiment 2) to take place at the surface. The initial emissions of ‘residual’ power plants, smeared
288 out over all industrial areas, are also emitted at the surface. However, we raise the height of the emissions to 20m
289 when these emissions are appointed to specific pixels. This height is representative for stack heights of small
290 power plants.

291 3 Results

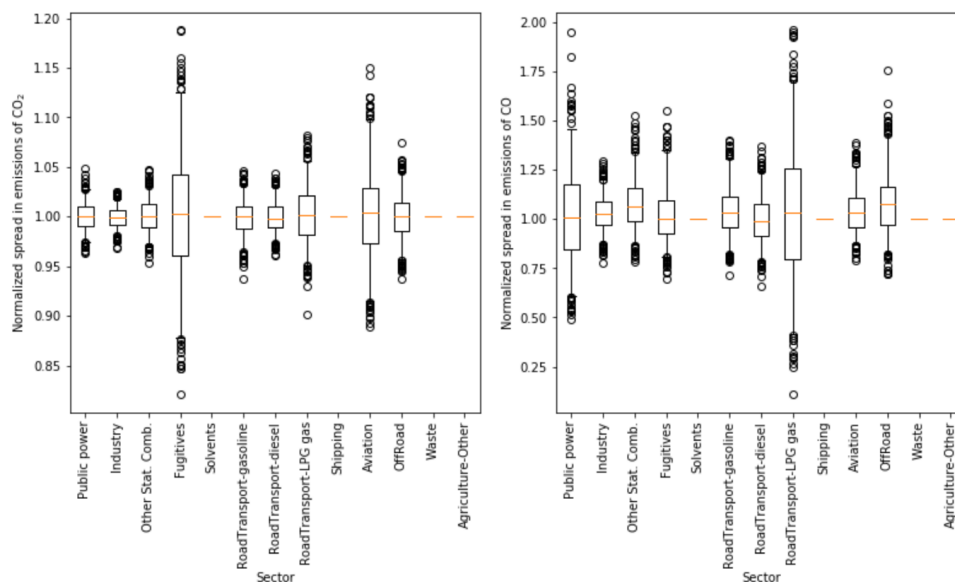
292 3.1 Uncertainties in total emissions

293 Using the uncertainties in emission factors and activity data we can evaluate the uncertainty in the total emissions
294 of CO₂ and CO per sector. Figure 7 shows the normalized spread in emissions per sector. The CO₂ emissions have
295 a relatively small uncertainty range and the uncertainty in the total emissions (all sectors together) is only about 1
296 % (standard deviation). The largest uncertainties are for fugitives and aviation, which are only small contributors
297 to the total CO₂ emissions (1.3 % and 0.4 %, respectively). Therefore, their contribution to the total emission
298 uncertainty is very small, as is shown in Figure 8. The largest uncertainty in the total CO₂ emissions is caused by
299 the public power sector. Despite the relatively small uncertainty in the emissions from this sector, it is the largest
300 contributor to the total CO₂ emissions (33 %) and therefore the uncertainty in the public power sector contributes
301 about 45 % to the uncertainty in the total CO₂ emissions.

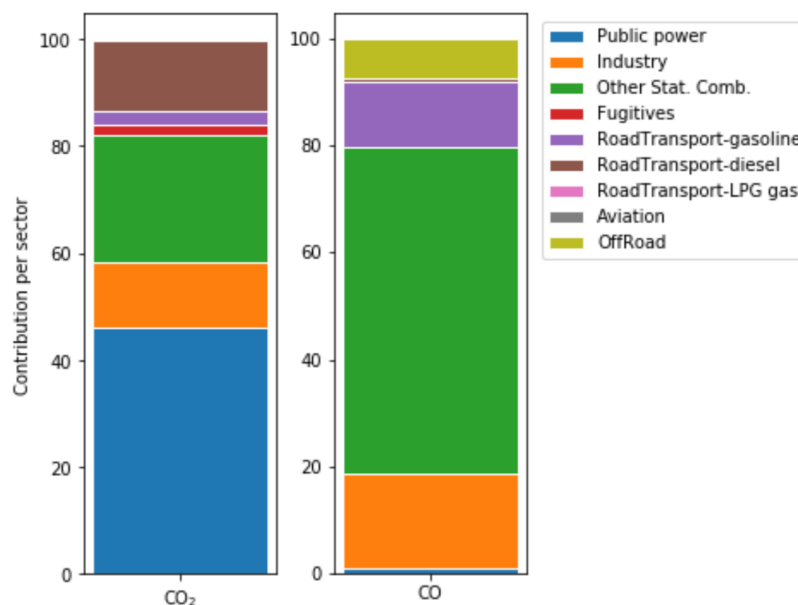
302 In contrast, the CO emissions show a larger uncertainty bandwidth with many high outliers caused by the
303 lognormal distribution of uncertainties in the emission factors. The uncertainty in the total emissions (all sectors
304 together) is 6 % for CO (standard deviation). Here, again the largest uncertainties are related to sectors (public



305 power and road transport (LPG fuel)) that are relatively small contributors to the total CO emissions. The main
 306 contributor to the uncertainty in total CO emissions is other stationary combustion, which contributes about 31 %
 307 to the total emissions and is responsible for more than 60 % of the total uncertainty.



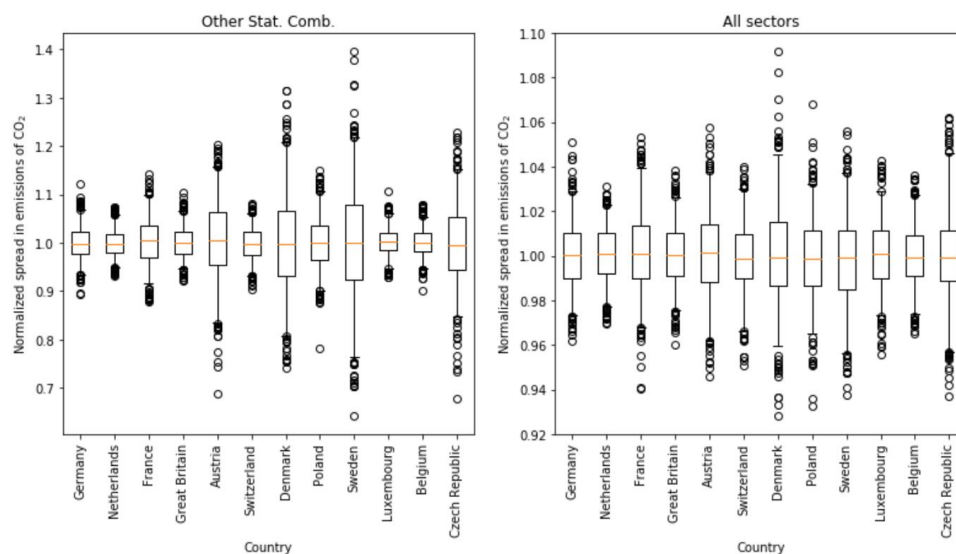
308
 309 **Figure 7: Normalized spread in emissions of CO₂ and CO.** The box represents the interquartile range, the whiskers the
 310 2.5–97.5 percentile, the lines the median values, and the circles are outliers. For sectors where no box is drawn there is
 311 no data included in the Monte Carlo simulation. Note the different scales of the y-axis.



312
 313 **Figure 8: Contribution of source sectors to the total uncertainty in CO₂ and CO emissions, summing to 100 %.**



314 Although the uncertainty in each parameter is assumed to be the same for each country, how a sector is composed
315 of sub-sectors can vary per country. Therefore, the uncertainty per aggregated sector can also vary per country.
316 An example is shown in Figure 9 (left panel), which shows the normalized spread in CO₂ emissions of other
317 stationary combustion for all countries within the domain. We find a much larger uncertainty in countries where
318 the relative fraction of biomass combustion is larger, because biomass burning has a much larger uncertainty in
319 both the activity data and the emission factor. For example, the percentage of biomass burning in the residential
320 sector is 54 % for the Czech Republic and 65 % for Denmark, compared to only 11 % and 9 % for the Netherlands
321 and Great Britain. Thus, differences in the fuel composition of countries result in differences in the overall
322 emission uncertainties, even if the uncertainty per parameter is estimated to be the same. Overall, the differences
323 between countries are relatively small (Figure 9, right panel).



324

325 **Figure 9: Normalized spread in emissions of CO₂ for other stationary combustion and all sectors combined for a range**
326 **of countries. The box represents the interquartile range, the whiskers the 2.5–97.5 percentile, the lines the median**
327 **values, and the circles are outliers.**

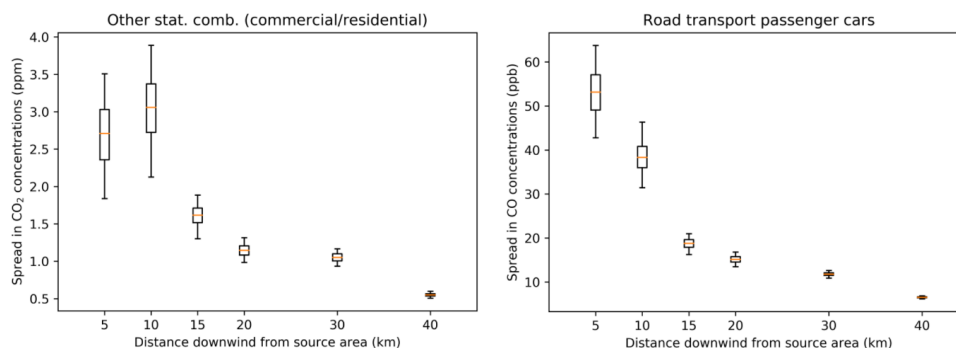
328 3.2 Uncertainties in spatial proxies

329 We examined the impact of uncertainties in spatial proxies on modelled CO₂ and CO concentrations for major
330 source sectors. For CO₂ we selected other stationary combustion (only commercial/residential, no
331 agriculture/forestry/fishing). The largest fraction (>90 %) of CO₂ emissions from this sector is distributed using
332 population density as proxy, which is used here (the remainder of the emissions is not considered). The uncertainty
333 in this sector-proxy combination is estimated to be 50% (normal distribution), mainly due to the disaggregation
334 to the 1x1 km resolution. For CO we selected road transport (all fuels, but only passenger cars). The spatial proxy
335 for distributing passenger car emissions is based on traffic intensities compiled using Open Transport Map and
336 Open Street Map, vehicle emission factors per road type/vehicle type/country, and fleet composition. The
337 uncertainty in this proxy is estimated to be 30 % (normal distribution) due to a higher intrinsic resolution.

338 Figure 10 shows the resulting spread in atmospheric concentrations as a function of downwind distance from the
339 source area. For CO₂ (left panel) we see a concentration of about 3.0 ppm at 10 km from the source area centre,



340 but with a large uncertainty bandwidth. This signal is large enough to measure, but with this large uncertainty
341 such measurements are difficult to use in an inversion. The measurement at 5 km from the source area centre is
342 slightly lower than the one at 10 km, because it is downwind of a part of the emissions. At longer distances, the
343 magnitude of the atmospheric signal decreases drastically, and so does the absolute spread in concentrations. The
344 signal becomes too small compared to the uncertainties occurring in a regular inversion framework to be useful.
345 The right panel shows a similar picture for the CO concentrations resulting from passenger car emissions. Again,
346 the spread in concentrations is large close to the source area centre and decreases with distance, but also the
347 magnitude of the signal decreases. Note that we focus here on a single source sector and the overall signals will
348 be larger and therefore easier to use. Nevertheless, the large spread in concentrations shows that a good
349 representation of the spatial distribution is important for constraining sectoral emissions.



350

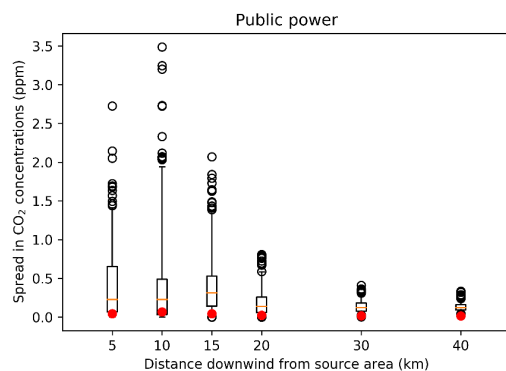
351 **Figure 10: Spread in concentrations of CO₂ resulting from commercial/residential emissions due to uncertainties in the**
352 **total population proxy map and spread in concentrations of CO resulting from road transport (passenger cars)**
353 **emissions due to uncertainties in the passenger cars proxy map. The box represents the interquartile range, the**
354 **whiskers the 2.5–97.5 percentile, and the lines the median values.**

355 Both proxy maps discussed here are the main proxy maps for the selected sectors. As mentioned before, some
356 sectors have residual emissions that are distributed using an alternative proxy map. An example is public power.
357 Large power plants are listed in databases, including the reported emissions (Table 3). The remainder of the
358 country emissions is spatially distributed over all industrial areas. However, it is more likely that the residual
359 emissions should be attributed to specific point sources (small power plants not listed in databases). That means
360 that instead of spreading the emissions over a large area, leading to very small local emissions and a low
361 concentration gradient, there could be relatively large emissions at a few locations. Therefore, the uncertainty in
362 these sector-proxy combinations is assumed to have a lognormal distribution, in part because of the absence of a
363 better estimation.

364 We illustrate the effect of this assumption by creating a new proxy map for residual (small) power plants. We find
365 that for the Netherlands a total capacity of 3655 MWe by 676 combustion plants is not included as a point source
366 (source: S&P Global Platts World Electric Power Plants database (<https://www.spglobal.com/platts/en/products-services/electric-power/world-electric-power-plants-database>)). At least 70 % of this capacity, attributed to 280
367 plants, is assumed to be in industrial areas. Given 4052 grid cells designated as industrial area in the Netherlands,
368 this is just 7 % of the total amount of industrial area grid cells assuming no more than one plant per grid cell. The
369 remainder is mainly related to cogeneration plants from glasshouses, which are located outside the industrial areas.
370 Therefore, we create a new proxy map for power plants by equally assigning 70 % of the emissions from the
371 residual power plants to 20 randomly chosen pixels (7 % of the total amount of industrial area pixels in the case
372



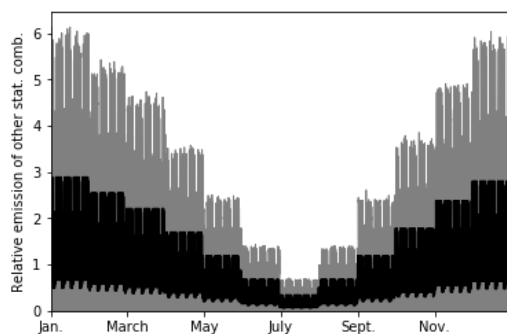
373 study area, i.e. the same density as for the Netherlands as a whole). As mentioned before, we also raise the height
374 of the emissions from surface level to 20 m, which is a better estimate of the stack height for small power plants.
375 The effect on local measurements is large (Figure 11). Instead of measuring a small and constant signal from this
376 sector, the assumed presence of small power plants results in measuring occasional large peak concentrations.
377 Thus, despite being relatively unimportant at the national level, for local studies the impact of the uncertainty in
378 these ‘residual’ proxies can be large.



379
380 **Figure 11: Spread in concentrations of CO₂ resulting from public power emissions due to differences in the proxy map:**
381 **emissions are distributed using the new proxy map with only 20 randomly chosen pixels containing emissions. The box**
382 **represents the interquartile range, the whiskers the 2.5–97.5 percentile, the lines the median values, and the black**
383 **circles are outliers. The red dots show concentrations of CO₂ when the original proxy map is used (industrial area).**

384 3.3 Uncertainties in time profiles

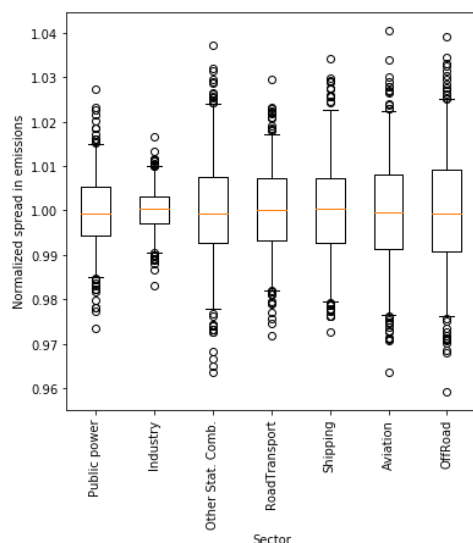
385 The timing of emissions is important to interpret measurements correctly. During morning rush hour, a peak is
386 expected in road traffic emissions, but the magnitude of this peak can differ from one day to the next. Also, the
387 seasonal cycle in emissions due to heating of buildings can vary between years due to varying weather conditions.
388 Yet, often fixed time profiles are used to describe the temporal disaggregation of annual emissions. The range of
389 possible values for the time profile of other stationary combustion is shown in Figure 12. The range can be very
390 large, especially during the winter. However, note that the average of each time profile is 1.0 for a full year, so
391 that the temporally distributed emissions add up to the annual total. Therefore, changes in the time profile indicate
392 shifts in the timing in the emissions and not changes in the overall emissions due to cold weather, which are
393 accounted for by the activity data.



394
395 **Figure 12: Spread in time profiles for other stationary combustion (N=500), resulting from the Monte Carlo simulation.**
396 **The black line represents the standard time profile.**



397 In inverse modelling, often well-mixed (non-stable) daytime measurements are selected, because these are least
398 prone to errors in model transport. The total annual emissions can then be calculated using a time profile. However,
399 if the time profile is not correct, an incorrect fraction of the emissions can be attributed to the selected hours. We
400 examined the impact of using an incorrect time profile on the total yearly emissions by calculating yearly
401 emissions for each ensemble member. Figure 13 shows the normalized spread in sectoral emissions for all
402 ensemble members. The error in the total annual emissions, resulting from the upscaling of daytime emissions
403 using an incorrect time profile, can reach up to about 1–2 %. This is a significant source of error for country-level
404 CO₂ emissions, but less important for CO as the other uncertainties for CO are much larger.



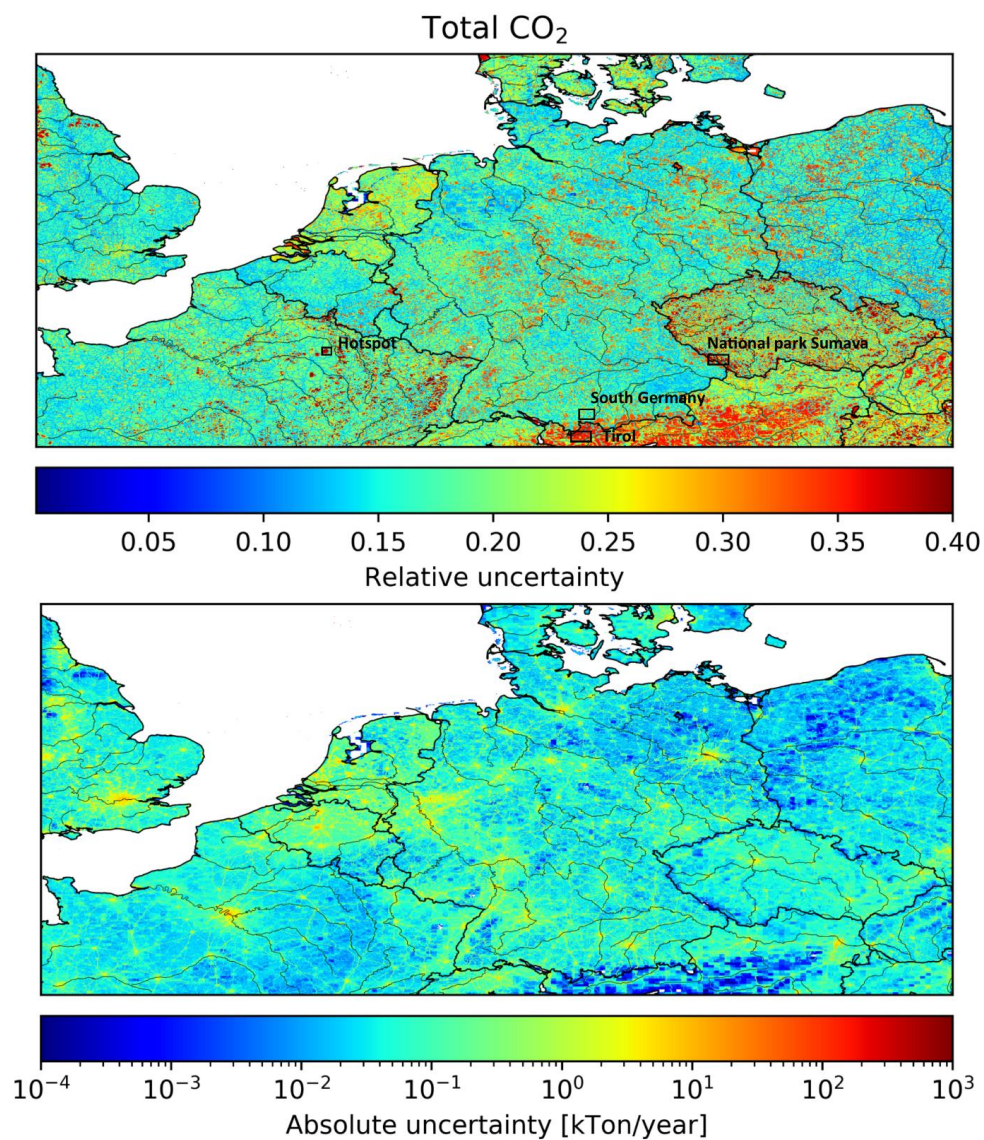
405

406 **Figure 13: Normalized spread in emissions per sector due to uncertainties in time profiles. The box represents the**
407 **interquartile range, the whiskers the 2.5–97.5 percentile, the lines the median values, and the circles are outliers.**

408 3.4 Uncertainty maps and spatial patterns

409 As mentioned before, the uncertainty of the emission value in a grid cell is determined by the uncertainties in
410 activity data, emission factors and spatial distribution proxies. The gridded uncertainty maps in Figure 14 and
411 Figure 15 illustrate that countries or (types of) regions differ significantly in their emission uncertainty, both in
412 absolute and relative values. Concerning the uncertainty in CO₂ and CO emissions, several observations can be
413 made.

414 First, for both CO and CO₂ the road network is visible due to low relative uncertainties and high absolute
415 uncertainties compared to the surroundings. This indicates that, despite having large emissions per pixel, the
416 spread in road traffic emissions among ensemble members is relatively small. This is likely due to the small
417 (normally distributed) uncertainty in the spatial proxies for road traffic, i.e. the location of the roads is well-known.
418 The surrounding rural areas are dominated by other stationary combustion, which has a slightly larger spatial
419 uncertainty.

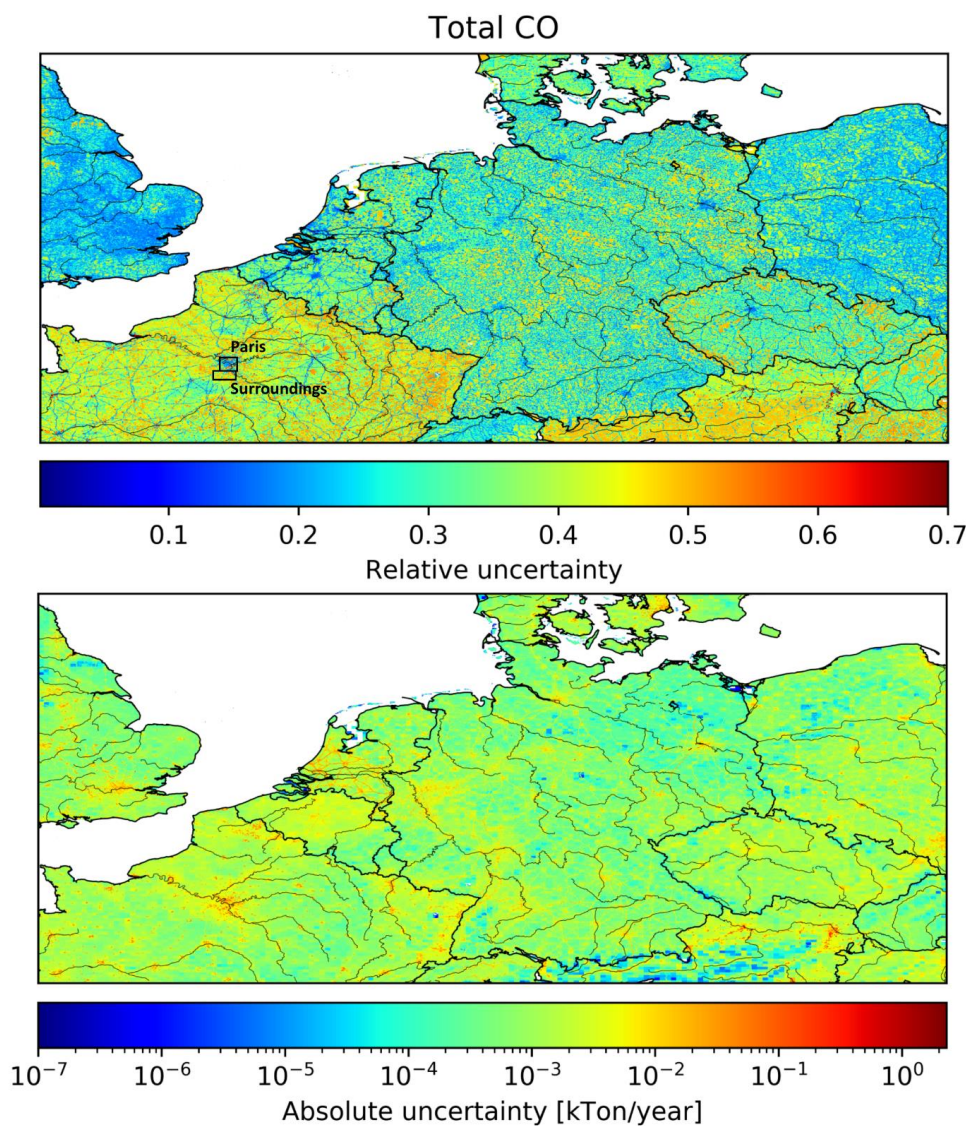


420

421

422

Figure 14: Maps of the relative and absolute uncertainty in CO₂ emissions. Areas that are examined in more detail are outlined by black squares in the top panel.



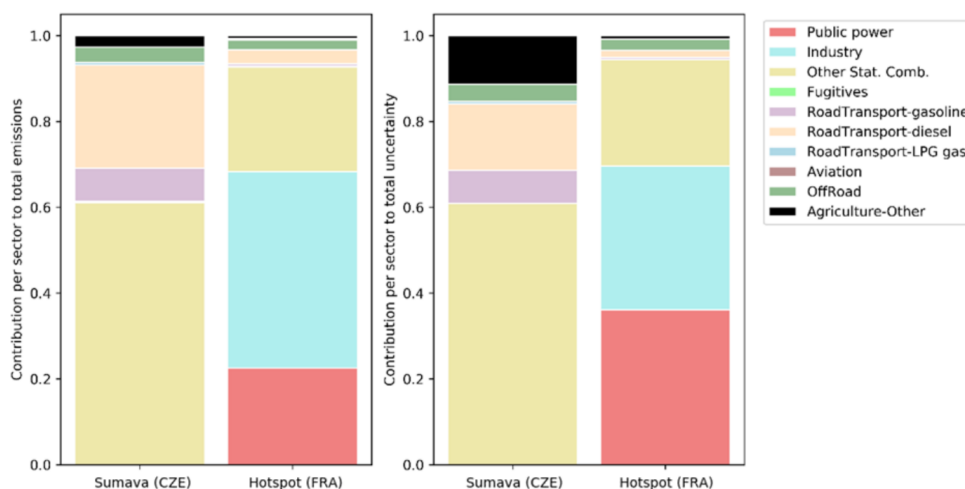
423

424 **Figure 15: Maps of the relative and absolute uncertainty in CO emissions. Areas that are examined in more detail are**
425 **outlined by black squares in the top panel.**

426 Second, in Austria (Tirol mainly) a large area of high relative uncertainty in CO₂ emissions is visible (average
427 pixel emission is 220 tonnes CO₂ yr⁻¹), which we compare to an area just on the other side of the border in southern
428 Germany (average pixel emission is 495 tonnes CO₂ yr⁻¹). The uncertainty in both areas is dominated by other
429 stationary combustion. Yet, in Austria a lot of biofuels are used (52 % of the total emissions for this source sector)
430 with a large uncertainty in the emission factor and spatial distribution, whereas in Germany only 20 % of the
431 emissions in this sector are caused by biofuels. On the other hand, the absolute uncertainty is very small in Tirol
432 because of the low population density (and thus small emissions) in this mountainous area.

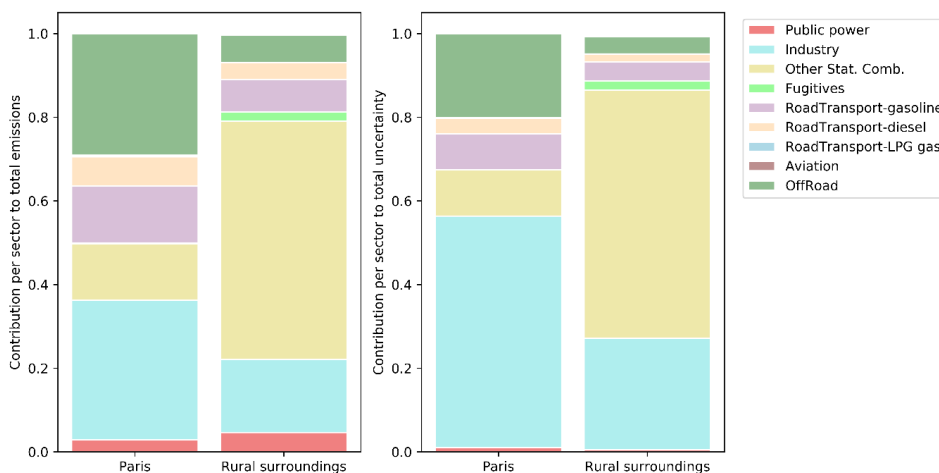


433 Third, some large patches of high relative uncertainty in CO₂ emissions are visible in the Czech Republic and
434 northeast France. The location of these patches seems to correspond to natural areas/parks. Therefore, absolute
435 uncertainties are low in these areas given the low emissions (average pixel emission in the Sumava national park
436 is 22 tonnes CO₂ yr⁻¹). The total uncertainty can be explained for 60 % by the uncertainty in other stationary
437 combustion, mainly wood burning (Figure 16). Also, agriculture (field burning of residues) plays a significant
438 role. In addition to these natural areas, there are also some very small dark red areas (relative uncertainty) in
439 northern France. These areas are military domain and have a lower absolute uncertainty than their surroundings
440 because very few emissions are distributed to these areas (average pixel emission is 250 tonnes CO₂ yr⁻¹). The
441 public power and industrial emissions are probably too small to be reported, hence the large relative uncertainty.
442



443
444 **Figure 16: Contribution of source sectors to the total emissions (left) and the total uncertainty (right) in CO₂ for the**
445 **Sumava national park in the Czech Republic and a hotspot in France, summing to 100 %. See Figure 14 for the exact**
446 **location of these areas.**

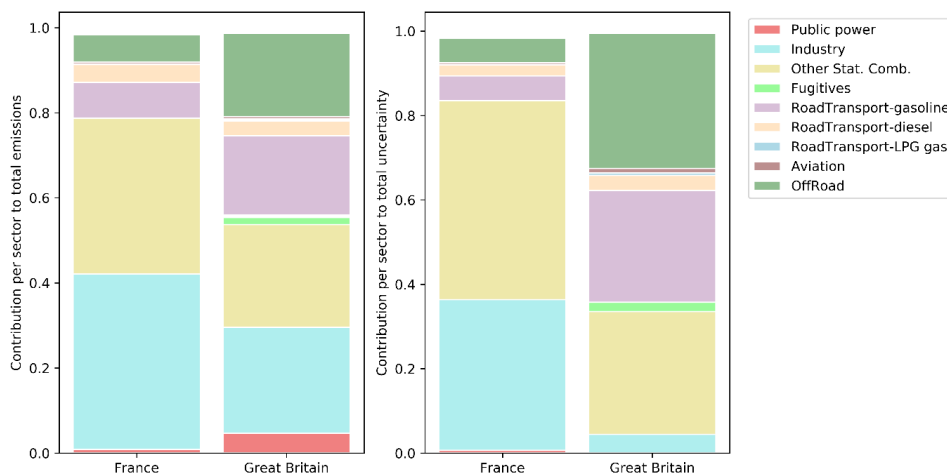
447 Fourth, big cities like Paris, Berlin and Brussels are clearly visible as areas where the relative uncertainty is lower
448 than in the surrounding areas. Compared to its surroundings, the uncertainty in Paris is mainly determined by the
449 industrial sector (Figure 17). Since industrial emissions are relatively well-known, the relative uncertainty is small.
450 However, the absolute uncertainty is large for big cities because of the high emissions in these densely populated
451 areas (average pixel emission is 64 tonnes CO yr⁻¹ for Paris). In the surrounding areas the emissions are again
452 dominated by other stationary combustion, which has a larger uncertainty. Yet, the absolute uncertainty is smaller
453 because of the lower emissions (average pixel emission is 12 tonnes CO yr⁻¹).



454

455 **Figure 17: Contribution of source sectors to the total emissions (left) and the total uncertainty (right) in CO for Paris**
456 **and its surroundings, summing to 100 %. See Figure 15 for the exact location of these areas.**

457 Finally, the relative uncertainties seem to be consistently higher in some countries than in others. For example,
458 the relative uncertainty in the total emissions of France and Great Britain (only pixels within the domain) are 39
459 % and 25 %, respectively. For France, the main sources of uncertainty are industry and other stationary
460 combustion, whereas the off-road and road transport sectors have a significant contribution to the uncertainty in
461 Great Britain (Figure 18). The main difference between the countries is again the amount of biomass used in the
462 other stationary combustion sector (26 % in France and 8 % in Great Britain). This is likely to explain why in
463 rural areas the relative uncertainty is much higher in France.



464

465 **Figure 18: Contribution of source sectors to the total emissions (left) and the total uncertainty (right) in CO for France**
466 **and Great Britain, summing to 100 %.**



467 **4. Discussion and conclusions**

468 Several previous studies have examined the uncertainty in emissions, either globally or nationally. For example,
469 Andres et al. (2014) studied the uncertainty in the CDIAC emission inventory on a global scale, suggesting that
470 the largest uncertainties are related to the fuel consumption (i.e. activity data). A similar concern was identified
471 for China, for which the uncertainty in energy statistics result in an uncertainty ratio of 15.6 % in the 2012 CO₂
472 emissions (Hong et al., 2017). In the present study the uncertainties in activity data and emission factors are similar
473 for CO₂, whereas the uncertainty in CO emission factors is much larger than the uncertainty in activity data. In
474 addition, many countries report uncertainties in emission estimates in their National Inventory Reports (UNFCCC,
475 2019). Yet, their methods differ and can even vary over time. Several scholars have examined the uncertainty in
476 national CO₂ emissions in more detail. For example, Monni et al. (2004) (Finland) and Fauster et al. (2011)
477 (Denmark) used a Tier 2 approach (Monte Carlo simulation) to determine the uncertainty in the total greenhouse
478 gas emissions. They found an uncertainty of about 5–6 % for the year 2001 for Finland and an uncertainty of 4–5
479 % for the year 2008 for Denmark, also considering non-normal distributions in uncertainties. Moreover, Oda et
480 al. (2019) found a 2.2 % difference in total CO₂ emissions in Poland between two emission inventories. These
481 values agree with our total emission uncertainties.

482 Even fewer studies have focused on uncertainties in the proxy maps used for spatial disaggregation. Some studies
483 compared emission inventories to get an idea of the spatial uncertainties (Gately and Hutyra, 2017; Hutchins et
484 al., 2017), but these studies are likely to underestimate uncertainties due to systematic errors caused when different
485 emission inventories use similar methods and/or proxies for spatial allocation. Moreover, exact quantification of
486 uncertainties is often limited, dependent on the spatial scale, and the uncertainties are not specified per source (i.e.
487 total emissions and spatial disaggregation) (Oda et al., 2019). Sowden et al. (2008) used a qualitative approach to
488 identify the uncertainty of different components of their emission inventory for reactive pollutants (activity,
489 emission factors, spatial and temporal allocation and speciation) by giving each component a quality rating. They
490 suggest that spatial allocation is an important source of uncertainty for residential burning, but not so much for
491 point sources and road traffic. Indeed, the location of large point sources and roads is relatively well-known.
492 However, we consider the allocation of emissions to pixels that include roads to have a significant (pixel value)
493 uncertainty. Therefore, our results show that uncertainties in the spatial proxy used for road traffic can cause a
494 significant spread in CO concentrations.

495 Andres et al. (2016) did a more extensive analysis of the spatial distribution in CDIAC, including uncertainties in
496 pixel values (e.g. due to incorrect accounting methods or changes over time) and due to the representativeness of
497 the proxy for the spatial distribution of emissions (also see Sect. 2.2.3). We considered these sources of uncertainty
498 as well. However, Andres et al. (2016) also mention spatial discretization as a source of error, because they assign
499 each pixel (1x1° resolution) to one country. The proxy maps used in this study include country fractions in each
500 pixel, reducing this uncertainty. In contrast, we suggest another source of uncertainty, namely the fact that some
501 pixels can include emissions while no activity takes place there or vice versa (proxy quality). Based on the listed
502 uncertainties, Andres et al. (2016) found an average uncertainty (2σ) in individual pixels of 120 % (assuming
503 normal distributions). Here, we find an average uncertainty (2σ) of 36 %. However, a small number of large
504 outliers occurs (less than 0.01 % of the pixels has an uncertainty of >1000 %) due to lognormal error distributions,
505 although these are related to pixels with small emissions. A large part of the difference can be explained by the
506 large pixel size of CDIAC and the large error introduced by spatial discretization (e.g. due to pixels that cover



507 large areas of two different countries). Also, their emissions are spatially distributed based on population density,
508 while we use a range of proxy maps depending on the source sector and use specific locations for large point
509 sources. However, the uncertainty estimates are partially based on expert judgement and remain subjective.
510 Moreover, the uncertainty related to the location of actual activities is not included in our uncertainty estimate,
511 even though we have shown this can have a large impact locally.

512 The country-level CO₂ emissions used for our emission inventory are based on NIR's, which are assumed to be
513 relatively accurate because of the use of detailed fuel consumption statistics and country-specific emission factors
514 (Andres et al., 2014; Francey et al., 2013). The uncertainties reported in the NIRs were determined following
515 specified procedures and are deemed the most complete and reliable estimates available. Yet, because of the use
516 of prescribed methods and in some cases general emission factors, systematic errors can occur both in the estimate
517 of parameters and in the estimate of uncertainties. We choose to average the uncertainties reported by several
518 countries, because the uncertainty estimates are relatively consistent across countries. However, this would not
519 eliminate such systematic errors. The effect of systematic errors could be analysed by comparing different sources
520 of information. Additionally, we assume point source emissions are relatively certain, yet a recent study showed
521 that significant uncertainties exist in reported emissions of US power plants (Quick and Marland, 2019). A similar
522 study for Europe is recommended, not only to improve the knowledge for the European situation, but also to
523 understand continental differences.

524 One source of uncertainty that is not considered in this study is the incompleteness of the emission inventory (i.e.
525 if sources are missing) or double-counting errors. For example, during the compilation of the base inventory we
526 found that in several cases the CO₂ emissions from airports were very low. The reason was that emissions from
527 international flights are not reported in the NIR's and therefore not part of the emission data used to create the
528 inventory. Once discovered, this was corrected and LTO (aircraft landing and take-off) emissions from
529 international flights were added in a later stage. Such discrepancies caused by reporting guidelines could be
530 present for other source types as well. Although overall this error is likely to be small, locally the errors might be
531 significant.

532 Finally, Sowden et al. (2008) mention (dis)aggregation as another source of error, i.e. the calculation of emissions
533 on a different scale (spatially, temporally or sector level) than the input data. In principle, fuel consumption data
534 is available on aggregated levels and then separated over different subsectors. This increases the uncertainty at
535 the lower level, but on the aggregated level the uncertainties remain the same. A similar note was made by Andres
536 et al. (2016) about the use of higher resolution proxy maps, which might increase the uncertainty due to lack of
537 local data. However, when local data is available this might also decrease the uncertainties. For example, the
538 EDGAR emission database uses non-country specific emission factors based on technology levels and sector
539 aggregated energy statistics (Muntean et al., 2018). The reason is that the level of detail we used in this paper is
540 not available globally. However, using generic emission factors can introduce large uncertainties when sub-
541 sectoral changes occur. Therefore, regional/local studies could benefit from using a dedicated emission inventory
542 for their region of interest instead of a global inventory.

543 In this work we studied the uncertainties in a high-resolution gridded emission inventory for CO₂ and CO,
544 considering uncertainties in the underlying parameters (activity data, emission factors, spatial proxy maps and
545 time profiles). We find that all factors play a significant role in determining the emission uncertainties, but that
546 the contribution of each factor differs per sector. Disaggregation of emissions introduces additional sources of



547 uncertainty, which makes uncertainties at higher resolution larger than at the scale of a country/year and can have
548 a large impact on (the interpretation of) local measurements. This is an important consideration for inverse
549 modelers and our methodology can be used to better define local uncertainties for e.g. urban inversions. Inverse
550 modelers should be aware that the use of erroneous time profiles to extrapolate emission data could result in errors
551 of a few percent. Moreover, we found that large regional differences exist in absolute and relative uncertainties.
552 By looking in more detail at specific regions (or countries) more insight can be gained about the emission
553 landscape and what are the main causes of uncertainty. Interestingly, areas with larger absolute uncertainties often
554 have smaller relative uncertainties. A likely explanation is that large sources of CO₂ and CO emissions received
555 more attention and are therefore relatively well-constrained, for example in the case of large point sources.
556 Nevertheless, since we are most interested in absolute emission reductions the map with absolute uncertainties
557 can be used to define an observational network that is able to reduce the largest absolute uncertainties. Finally,
558 we believe that an uncertainty product based on a well-defined, well-documented and systematic methodology
559 could be beneficial for the entire modelling community and support decision-making as well. However, specific
560 needs can differ significantly between studies, for example the scale/resolution, source sector aggregation level,
561 and which species are included. Therefore, the creation of a generic uncertainty product is challenging and needs
562 further research.

563 **Data availability**

564 The emission inventories are available for non-commercial applications and research. Please contact Hugo Denier
565 van der Gon (hugo.deniervandergon@tno.nl).



Appendix A

Table A1: Relative uncertainties (fraction) in activity data and CO₂ emission factors as taken from the NIRs (country-average) and in CO emission factors as derived from literature (assumed equal for all countries in the domain). The quoted uncertainty ranges are assumed to be representative for one standard deviation. Uncertainties in activity data and CO₂ emission factors are often relatively low and symmetrically distributed and normal distributions (Norm) are assumed for these activities. Compared to CO₂ emission factors, the uncertainty in CO emission factors is much higher, up to an order of magnitude. Uncertainties in CO emission factors are often lognormally distributed (Logn) and are assumed equal for all countries in the HR domain. The uncertainty in the activity of open burning of waste (not covered by the NIRs) is also assumed to have a lognormal distribution.

Sector (NFR)	Fuel type	Activity data		CO ₂ emission factors		CO emission factors	
		Average	Distribution	Average	Distribution	Average	Distribution
Public electricity and heat production (1.A.1.a)	Solid (fossil)	0.018	Norm	0.030	Norm	0.149	Logn
	Liquid (fossil)	0.022	Norm	0.031	Norm	0.399	Norm
	Gaseous (fossil)	0.021	Norm	0.015	Norm	0.513	Norm
	Biomass	0.060	Norm	0.05	Norm	0.231	Logn
Oil and gas refining (1.A.1.b & 1.B.2.d)	All	0.038	Norm	0.048	Norm	0.402	Norm
Oil production & Gas exploration (1.B.2 mainly flaring, 1.B.2.c)	All	0.118	Norm	0.141	Norm	0.240	Logn
Iron and steel industry (1.A.2.a & 2.C.1)	All	0.044	Norm	0.056	Norm	0.240	Logn
Non-ferrous metals (1.A.2.b & 2.C.2_3)	All	0.031	Norm	0.029	Norm	0.208	Norm
Chemical industry (1.A.2.c & 2.B)	All	0.042	Norm	0.041	Norm	0.138	Logn
Pulp and paper industry (1.A.2.d)	All	0.027	Norm	0.016	Norm	0.138	Logn
Food processing, beverages and tobacco (1.A.2.e)	All	0.029	Norm	0.017	Norm	0.138	Logn
Non-metallic minerals (1.A.2.f & 2.A)	All	0.032	Norm	0.041	Norm	0.384	Logn
Other manufacturing industry (1.A.2.g)	All	0.029	Norm	0.014	Norm	0.138	Logn
Civil aviation - LTO (1.A.3.a)	All	0.089	Norm	0.040	Norm	0.231	Logn
Road transport (all vehicle types) (1.A.3.b)	Gasoline (fossil)	0.031	Norm	0.025	Norm	0.284	Logn
	Diesel (fossil)	0.032	Norm	0.026	Norm	0.319	Norm
	Gaseous (fossil)	0.039	Norm	0.027	Norm	0.320	Logn
	LPG	0.039	Norm	0.027	Norm	0.462	Norm
Other transport (1.A.3.e & 1.A.4 mobile)	All	0.067	Norm	0.023	Norm	0.384	Logn
Other mobile (1.A.5.b)	All	0.098	Norm	0.026	Norm	0.384	Logn
Residential (1.A.4.b)	Gaseous (fossil)	0.040	Norm	0.022	Norm	0.141	Logn
	Liquid (fossil)	0.048	Norm	0.024	Norm	0.404	Norm
	Solid (fossil)	0.085	Norm	0.041	Norm	0.141	Logn
	Biomass	0.163	Norm	0.055	Norm	0.384	Logn
Commercial institutional (1.A.4.a)	Gaseous (fossil)	0.043	Norm	0.022	Norm	0.138	Logn
	Liquid (fossil)	0.055	Norm	0.023	Norm	1.065	Norm
	Solid (fossil)	0.087	Norm	0.040	Norm	0.994	Norm
	Biomass	0.103	Norm	0.055	Norm	0.730	Logn



Agriculture/Forestry/Fishing (1.A.4.c)	Gaseous (fossil)	0.050	Norm	0.028	Norm	0.138	Logn
	Liquid (fossil)	0.051	Norm	0.029	Norm	1.065	Norm
	Solid (fossil)	0.095	Norm	0.048	Norm	0.994	Norm
	Biomass	0.096	Norm	0.09	Norm	0.730	Logn
Other stationary (1.A.5.a)	Gaseous (fossil)	0.097	Norm	0.023	Norm	0.138	Logn
	Liquid (fossil)	0.084	Norm	0.021	Norm	1.065	Norm
	Solid (fossil)	0.103	Norm	0.033	Norm	0.994	Norm
	Biomass	0.180	Norm	0.04	Norm	0.730	Logn
Agricultural waste burning (3.F)	-	1.609	Logn	0.2	Norm	0.429	Norm
Uncontrolled waste burning (5.C.2)	-	1.609	Logn	0.5	Norm	0.366	Logn

Table A2: Relative uncertainties (fractions) at cell level resulting from the spatial distribution. The values listed represent the (one standard deviation) uncertainty of the emission per cell due to uncertainty sources 2 and 3 as listed in Sect. 2.2.3. All values in the table below are based on expert quantification and inevitably include a considerable amount of subjectivity. The data should therefore be considered as a first order indication only. Note that the natural logarithm (Ln) of the uncertainty fraction is given in case uncertainty has a lognormal distribution.

Sector name	Proxy name	Distribution	Uncertainty
Public electricity and heat production; Chemical industry; Food processing, beverages and tobacco (comb); Food and beverages industry; Other non-metallic mineral production; Small combustion - Commercial/institutional – Mobile	CORINE_2012_Industrial_area	Logn	2.2
Solid fuel transformation; Iron and steel industry (comb); Iron and steel production; Pulp and paper industry (comb); Pulp and paper industry; Non-metallic minerals (comb); Cement production	CORINE_2012_Industrial_area	Logn	3.7
Other manufacturing industry (comb); Other industrial processes; Manufacturing industry - Off-road vehicles and other machinery	CORINE_2012_Industrial_area	Logn	1.4
Oil and gas refining (comb); Oil and gas refining	CORINE_2012_Industrial_area	Logn	3.7
	TNO_PS for Refineries	Logn	1.7
Coal mining (comb)	CORINE_2012_Industrial_area	Logn	4.6
	TNO_PS for Coal mining	Logn	1.7
Oil production (comb)	CORINE_2012_Industrial_area	Logn	1.7
	TNO_PS for Oil production	Logn	1.7
Gas exploration (comb)	CORINE_2012_Industrial_area	Logn	1.7
	TNO_PS for Gas production	Logn	1.7
Coke ovens (comb)	CORINE_2012_Industrial_area	Logn	1.7
	TNO_PS for Iron and steel - Coke ovens	Logn	1.7
Non-ferrous metals (comb); Other non-ferrous metal production	CORINE_2012_Industrial_area	Logn	3.7
	TNO_PS for Non-ferrous metals - Other	Logn	1.7
Aluminium production	CORINE_2012_Industrial_area	Logn	3.7
	TNO_PS for Non-ferrous metals - Aluminium	Logn	1.7
Chemical industry (comb)	CORINE_2012_Industrial_area	Logn	2.2
	TNO_PS for Chemical industry	Logn	1.7
Passenger cars	RoadTransport_PassengerCars	Norm	0.3
Light duty vehicles	RoadTransport_LightCommercialVehicles	Norm	0.3
Trucks (>3.5t)	RoadTransport_HeavyDutyTrucks	Norm	0.3



Buses	RoadTransport_Buses	Norm	0.3
Motorcycles	RoadTransport_Motorcycles	Norm	0.3
Mopeds	RoadTransport_Mopeds	Norm	0.5
Civil aviation – LTO	Airport distribution for year 2015	Logn	1.4
Mobile sources in agriculture/forestry/fishing	CORINE_2012_Arable_land	Logn	1.4
Other transportation, including pipeline compressors	Population_total_2015	Logn	3.7
Small combustion - Residential - Household and gardening; Other mobile combustion	Population_total_2015	Logn	1.3
Commercial/institutional	Population_total_2015	Norm	0.5
	Population_rural_2015	Logn	1.3
	Population_urban_2015	Logn	1.3
	Wood_use_2014	Logn	2.2
Residential	Population_total_2015	Norm	0.5
	Population_rural_2015	Logn	1.3
	Population_urban_2015	Logn	1.3
	Wood_use_2014	Logn	1.4
Agriculture/Forestry/Fishing	CORINE_2012_Arable_land	Logn	1.4
	Wood_use_2014	Logn	2.2
Other stationary combustion	Population_total_2015	Logn	1.3
	Population_rural_2015	Logn	1.3
	Wood_use_2014	Logn	1.4
Field burning of agricultural residues	CORINE_2012_Arable_land	Logn	2.2
	Population_total_2015	Logn	2.2
Open burning of waste	CORINE_2012_Industrial_area	Logn	3.7
	Population_rural_2015	Logn	3.7

Author contribution

A.J.H. Visschedijk assembled the uncertainty data used in this work. S.N.C. Dellaert and H.A.C. Denier van der Gon are responsible for the base emission inventory. I. Super designed the experiments, carried them out, and prepared the manuscript with contributions from all co-authors.

Competing interests

The authors declare that they have no conflict of interest.

Acknowledgements

This study was supported by the CO₂ Human Emissions (CHE) project, funded by the European Union's Horizon 2020 research and innovation programme under grant agreement No 776186 and the VERIFY project, funded by the European Union's Horizon 2020 research and innovation programme under grant agreement No 776810.

References

Amann, M., Bertok, I., Borcken-Kleefeld, J., Cofala, J., Heyes, C., Höglund-Isaksson, L., Klimont, Z., Nguyen, B., Posch, M., Rafaj, P., Sandler, R., Schöpp, W., Wagner, F. and Winiwarter, W.: Cost-effective control of air



- quality and greenhouse gases in Europe: Modeling and policy applications, *Environ. Model. Softw.*, 26, 1489–1501, doi:<https://doi.org/10.1016/j.envsoft.2011.07.012>, 2011.
- Andres, R. J., Boden, T. A. and Higdon, D.: A new evaluation of the uncertainty associated with CDIAC estimates of fossil fuel carbon dioxide emission, *Tellus, Ser. B Chem. Phys. Meteorol.*, 66, doi:<https://doi.org/10.3402/tellusb.v66.23616>, 2014.
- Andres, R. J., Boden, T. A. and Higdon, D. M.: Gridded uncertainty in fossil fuel carbon dioxide emission maps, a CDIAC example, *Atmos. Chem. Phys.*, 16, 14979–14995, doi:<https://doi.org/10.5194/acp-16-14979-2016>, 2016.
- Berner, R. A.: The long-term carbon cycle, fossil fuels and atmospheric composition, *Nature*, 426, 323–326, doi:<https://doi.org/10.1038/nature02131>, 2003.
- Boschetti, F., Thouret, V., Maenhout, G. J., Totsche, K. U., Marshall, J. and Gerbig, C.: Multi-species inversion and IAGOS airborne data for a better constraint of continental-scale fluxes, *Atmos. Chem. Phys.*, 18, 9225–9241, doi:<https://doi.org/10.5194/acp-18-9225-2018>, 2018.
- Denier van der Gon, H. A. C., Hendriks, C., Kuenen, J., Segers, A. and Visschedijk, A.: Description of current temporal emission patterns and sensitivity of predicted AQ for temporal emission patterns, TNO, Utrecht., 2011.
- Denier van der Gon, H. A. C., Kuenen, J. J. P., Janssens-Maenhout, G., Döring, U., Jonkers, S. and Visschedijk, A.: TNO_CAMS high resolution European emission inventory 2000–2014 for anthropogenic CO₂ and future years following two different pathways, *Earth Syst. Sci. Data Discuss.*, 2017, 1–30, doi:<https://doi.org/10.5194/essd-2017-124>, 2017.
- European Environment Agency: EMEP/EEA air pollutant emission inventory guidebook 2016: Technical guidance to prepare national emission inventories, Luxembourg., 2016.
- Fauster, P., Sørensen, P. B., Nielsen, M., Winther, M., Plejdrup, M. S., Hoffmann, L., Gyldenørne, S., Mikkelsen, H. M., Albrektsen, R., Lyck, E., Thomsen, M., Hjelgaard, K. and Nielsen, O.-K.: Monte Carlo Tier 2 uncertainty analysis of Danish Greenhouse gas emission inventory, *Greenh. Gas Meas. Manag.*, 145–160, doi:<https://doi.org/10.1080/20430779.2011.621949>, 2011.
- Francey, R. J., Trudinger, C. M., Van der Schoot, M., Law, R. M., Krummel, P. B., Langenfelds, R. L., Paul Steele, L., Allison, C. E., Stavert, A. R., Andres, R. J. and Rödenbeck, C.: Atmospheric verification of anthropogenic CO₂ emission trends, *Nat. Clim. Chang.*, 3, 520–524, doi:<https://doi.org/10.1038/nclimate1817>, 2013.
- Gately, C. K. and Hutyrá, L. R.: Large uncertainties in urban-scale carbon emissions, *J. Geophys. Res. Atmos.*, 122, doi:<https://doi.org/10.1002/2017JD027359>, 2017.
- Gurney, K. R., Zhou, Y., Mendoza, D., Chandrasekaran, V., Geethakumar, S., Razlivanov, I., Song, Y. and Godbole, A.: Vulcan and Hestia: High resolution quantification of fossil fuel CO₂ emissions, in: MODSIM 2011 - 19th International Congress on Modelling and Simulation - Sustaining Our Future: Understanding and Living with Uncertainty, pp. 1781–1787., 2011.
- Gurney, K. R., Patarasuk, R., Liang, J., Song, Y., Keeffe, D., Rao, P., Whetstone, J. R., Duren, R. M., Elderling, A. and Miller, C.: The Hestia fossil fuel CO₂ emissions data product for the Los Angeles megacity (Hestia-LA), *Earth Syst. Sci. Data Discuss.*, 2030, 1–38, doi:<https://doi.org/10.5194/essd-2018-162>, 2019.
- Hong, C., Zhang, Q., He, K., Guan, D., Li, M., Liu, F. and Zheng, B.: Variations of China's emission estimates: Response to uncertainties in energy statistics, *Atmos. Chem. Phys.*, 17, 1227–1239,



doi:<https://doi.org/10.5194/acp-17-1227-2017>, 2017.

Hutchins, M. G., Colby, J. D., Marland, G. and Marland, E.: A comparison of five high-resolution spatially-explicit, fossil-fuel, carbon dioxide emission inventories for the United States, *Mitig. Adapt. Strat. Gl.*, 22, 947–972, doi:<https://doi.org/10.1007/s11027-016-9709-9>, 2017.

IEA: World Energy Outlook 2008, Paris., 2008.

Van Jaarsveld, J. A.: The Operational Priority Substances model. Description and validation of OPS-Pro 4.1, Bilthoven., 2004.

Kuennen, J. J. P., Visschedijk, A. J. H., Jozwicka, M. and Denier van der Gon, H. A. C.: TNO-MACC-II emission inventory; A multi-year (2003-2009) consistent high-resolution European emission inventory for air quality modelling, *Atmos. Chem. Phys.*, 14, 10963–10976, doi:<https://doi.org/10.5194/acp-14-10963-2014>, 2014.

Monni, S., Syri, S. and Savolainen, I.: Uncertainties in the Finnish greenhouse gas emission inventory, *Environ. Sci. Policy*, 7, 87–98, doi:<https://doi.org/10.1016/j.envsci.2004.01.002>, 2004.

Muntean, M., Vignati, E., Crippa, M., Solazzo, E., Schaaf, E., Guizzardi, D. and Olivier, J. G. : Fossil CO₂ emissions of all world countries - 2018 report, Luxembourg., 2018.

Oda, T., Bun, R., Kinakh, V., Topylko, P., Halushchak, M., Marland, G., Lauvaux, T., Jonas, M., Maksyutov, S., Nahorski, Z., Lesiv, M., Danylo, O. and Joanna, H.-P.: Errors and uncertainties in a gridded carbon dioxide emissions inventory, *Mitig. Adapt. Strateg. Glob. Chang.*, doi:<https://doi.org/10.1007/s11027-019-09877-2>, 2019.

Palmer, P. I., O'Doherty, S., Allen, G., Bower, K., Bösch, H., Chipperfield, M. P., Connors, S., Dhomse, S., Feng, L., Finch, D. P., Gallagher, M. W., Gloor, E., Gonzi, S., Harris, N. R. P., Helfter, C., Humpage, N., Kerridge, B., Knappett, D., Jones, R. L., Le Breton, M., Lunt, M. F., Manning, A. J., Matthesen, S., Muller, J. B. A., Mullinger, N., Nemitz, E., O'Shea, S., Parker, R. J., Percival, C. J., Pitt, J., Riddick, S. N., Rigby, M., Sembhi, H., Siddans, R., Skelton, R. L., Smith, P., Sonderfeld, H., Stanley, K., Stavert, A. R., Wenger, A., White, E., Wilson, C. and Young, D.: A measurement-based verification framework for UK greenhouse gas emissions: an overview of the Greenhouse gAs UK and Global Emissions (GAUGE) project, *Atmos. Chem. Phys.*, 18, 11753–11777, doi:<https://doi.org/10.5194/acp-18-11753-2018>, 2018.

Quick, J. C. and Marland, E.: Systematic error and uncertain carbon dioxide emissions from USA power plants, *J. Air Waste Manage. Assoc.*, 2247, doi:<https://doi.org/10.1080/10962247.2019.1578702>, 2019.

Sauter, F., Van Zanten, M., Van der Swaluw, E., Aben, J., De Leeuw, F. and Van Jaarsveld, H.: The OPS-model. Description of OPS 4.5.0, Bilthoven., 2016.

Sowden, M., Cairncross, E., Wilson, G., Zunckel, M., Kirillova, E., Reddy, V. and Hietkamp, S.: Developing a spatially and temporally resolved emission inventory for photochemical modeling in the City of Cape Town and assessing its uncertainty, *Atmos. Environ.*, 42, 7155–7164, doi:<https://doi.org/10.1016/j.atmosenv.2008.05.048>, 2008.

Super, I., Denier van der Gon, H. A. C., Van der Molen, M. K., Sterk, H. A. M., Hensen, A. and Peters, W.: A multi-model approach to monitor emissions of CO₂ and CO from an urban-industrial complex, *Atmos. Chem. Phys.*, 17, doi:<https://doi.org/10.5194/acp-17-13297-2017>, 2017a.

Super, I., Denier van der Gon, H. A. C., Visschedijk, A. J. H., Moerman, M. M., Chen, H., van der Molen, M. K. and Peters, W.: Interpreting continuous in-situ observations of carbon dioxide and carbon monoxide in the urban port area of Rotterdam, *Atmos. Pollut. Res.*, 8, doi:<https://doi.org/10.1016/j.apr.2016.08.008>, 2017b.

UNFCCC: National Inventory Submissions 2019, [online] Available from: <https://unfccc.int/process-and->



meetings/transparency-and-reporting/reporting-and-review-under-the-convention/greenhouse-gas-inventories-annex-i-parties/national-inventory-submissions-2019, 2019.

Zheng, B., Chevallier, F., Yin, Y., Ciais, P., Fortems-cheiney, A., Deeter, M. N., Parker, R. J., Wang, Y., Worden, H. M. and Zhao, Y.: Global atmospheric carbon monoxide budget 2000–2017 inferred from multi-species atmospheric inversions, *Earth Syst. Sci. Data Discuss.*, 1, 1–42, doi:<https://doi.org/10.5194/essd-2019-61>, 2019.